A πCI approach to the study of correlation effects on the nonlinearoptical properties in organic πconjugated systems

I. D. L. Albert, J. O. Morley, and D. Pugh

Citation: The Journal of Chemical Physics **102**, 237 (1995); doi: 10.1063/1.469396
View online: http://dx.doi.org/10.1063/1.469396
View Table of Contents: http://scitation.aip.org/content/aip/journal/jcp/102/1?ver=pdfcov
Published by the AIP Publishing

A πCI approach to the study of correlation effects on the nonlinear-optical properties in organic π-conjugated systems

I. D. L. Albert
Department of Pure and Applied Chemistry, University of Strathclyde, 295 Cathedral Street, Glasgow G1 1XL, United Kingdom

J. O. Morley
Department of Chemistry, University College of Swansea, Singleton Park, Swansea SA2 8PP, United Kingdom

D. Pugh
Department of Pure and Applied Chemistry, University of Strathclyde, 295 Cathedral Street, Glasgow G1 1XL, United Kingdom

(Received 23 June 1994; accepted 22 September 1994)

A π-electron method which allows for the systematic inclusion of configuration interaction of any order has been developed for the computation of electronic and optical properties of conjugated molecules. It has been used to study the effect of electron correlation on these properties in all *trans* finite polyenes of up to 16 carbon atoms. For smaller molecules it has been possible to carry out a complete set of CI calculations, from singly excited (SCI) to full configuration interaction (FCI). For the larger molecules the SCI and doubly excited CI (SDCI) calculations have been performed. The program permits the execution of a configuration interaction calculation of any order, n, in which all configurations involving the excitation of 1,2,...,n electrons from the occupied π-orbitals of the Hartree–Fock ground-state to the virtual π-orbitals are included. The set of π-orbitals is extracted from the ground state obtained from an all valence-electron, complete neglect of differential overlap (CNDO) calculation. The configurations are represented by binary integers so that their generation and storage is very rapid and efficient. The nonlinear optical properties have been computed mainly by the correction vector method but in some cases the sum-over-states (SOS) method has also been used to study the evolution of the THG coefficient as virtual states of increasing energy are added. The results obtained for the finite polyenes are found to be in very good agreement with both experimental and other theoretical values in literature. The results clearly show the effect of electron correlation, which is found to affect the electronic and optical properties of these systems both qualitatively and quantitatively.

I. INTRODUCTION

Organic molecules with extended π-conjugation have been of special interest to chemists, physicists, and biologists for a number of reasons. On excitation these molecules undergo a variety of photochemical reactions that are of importance in biological systems. As examples we may cite the mechanisms of photosynthesis in plants and vision in animals as two important instances where excited states of conjugated molecules are involved. The essential moiety in the photochemical reaction involved in photosynthesis is the porphyrin group in chlorophyll, which is a macrocyclic conjugated system. One of the carotenoids, 11-*cis*-retinal, is the chromophore of the visual pigment rhodopsin in animals and it has now been well established that the primary process in vision arises from the *cis–trans* photoisomerization reaction that occurs when 11-*cis*-retinal, an aldehyde formed from the linear polyene, is irradiated with light. The isomerization of 11-*cis*-retinal to its *trans* form leads to a charge separation and this is assumed to pass an electric signal to opsin, the protein component of rhodopsin, which is thought to be the neural event originating the process of vision.[1,2]

A variety of physical properties, determined primarily by the delocalized π-electrons, have also been successfully exploited in electronic and optical applications of the polyenes. For example, the pristine polyenes, which are intrinsic semiconductors with a band gap of 2 eV, when doped with suitable donors and acceptors have conductivities that rival those of Cu.[3] Little envisaged the possibility of a room temperature superconducting material with a conducting conjugated π-backbone to which polarizable side groups are attached.[4] Although there are no current examples of room temperature superconductors formed from these materials $(BEDT\text{-}TTF)_2X$ salts are known to exhibit superconducting properties at a lower temperature.[5,6] Furthermore, organic π-conjugated molecules show unusually large ultrafast nonresonant macroscopic second and third order nonlinear optical susceptibilities.[7–10] Organic systems substituted with donor and acceptor groups possess second order coefficients which are much larger than those of the conventional inorganics such as $LiNbO_4$ or KH_2PO_4.

The entirely electronic nature of the effect in organic materials ensures the ultrafast response times and low dielectric constants essential for device applications. Systems with a center of inversion such as the unsubstituted polyenes exhibit large third order nonlinearities.

For a satisfactory understanding of the electronic and optical properties of conjugated systems a detailed knowledge of their electronic states is a prerequisite. There have been a number of reports on the quantum mechanical de-

 0021-9606/95/102(1)/237/14/$6.00

scription of the electronic states of these compounds and their relations to their chemical and physical properties. The major outcome of these studies is the clear demonstration of the importance of electron correlation.[11–13] Some of the manifest consequences of strong correlations are to be seen in the existence of dipole unallowed states below the lowest dipole allowed state,[14,15] in the finite optical gaps of infinite polyenes, and in the presence of negative spin densities at the even numbered carbon sites of neutral polyene radicals.[16,17] It is well established that a ^1A_g state, a state of the same symmetry as the ground state, exists below the lowest dipole allowed ^1B_u state in the finite polyenes and that a $^1E_{2g}$ state occurs below the optical allowed $^1E_{1u}$ state in benzene.

In the semiempirical quantum theory of excited electronic states it is found that an adjustment of certain key integrals leads to the reproduction of some experimental results. This adjustment itself is equivalent to the introduction of some electron correlation, but a treatment that introduces correlation explicitly through configuration interaction is found to be necessary if an adequate account of properties of the excited state energy level system, such as those described in the preceding paragraph, is to be obtained.[18–22] The results of calculations on the unsubstituted polyenes that explicitly take into account electron correlation are markedly different, both qualitatively and quantitatively, from those that do not.

There have been a number of reports on the importance of virtual two photon states in determining the magnitude and sign of the second hyperpolarizability of conjugated systems.[19–22] For example the importance of a virtual two photon ^1A_g state above the dipole allowed ^1B_u state in determining the sign and magnitude of the third harmonic generation (THG) coefficient of 1,3,5,7-*all trans*-octatetraene has been recognized by Garito *et al.*,[21] Soos and Ramasesha,[19] and Pierce.[22] Soos and Ramasesha have obtained their result from a full CI calculation within the chosen PPP model Hamiltonian, while Garito *et al.* and Pierce have reached a similar conclusion using limited CI calculations. Our earlier studies[20] on the NLO coefficients of polyenes of up to 10 carbon atoms using a πSDCI (singly and doubly excited configuration interaction) calculation within the CNDO approximation also produced similar results. Although these studies indicate that correlations at the level of SDCI are sufficient to reproduce many of the experimental results of smaller polyenes, it has been emphasized by Tavan and Schulten[18] that correlations of higher order have to taken into account when treating polyenes longer than octatetraene.

In this paper we investigate the effect, on the calculated polyene NLO properties, of increasing the order of configuration interaction in a systematic way and the important effects of electron correlation in conjugated systems are demonstrated. Finite polyenes of up to sixteen carbon atoms, for which there are a number of experimental and theoretical results on electronic and optical properties available for comparison, have been chosen for the present study. In the next section we briefly review the method of configuration interaction and describe in more detail an efficient method of performing full and limited configuration interaction calculations using the CNDO Hamiltonian.[23] In Sec. III we present the results of our calculations on the electronic, linear and nonlinear optical properties of some of the π-conjugated systems and discuss them in the context of the origin of the large NLO response in these systems.

II. COMPUTATIONAL DETAILS

Two major approaches exist in quantum chemistry for the treatment of electron correlation;[24] (1) the perturbation theoretical approach; and (2) the configuration interaction (CI) method. In the perturbative approach, the total Hamiltonian of the system is partitioned into two parts, the zeroth order part H_0 and a perturbation V. H_0 is chosen such that the eigenfunctions and eigenvalues are known and the exact energy is expressed as an infinite sum of contributions of increasing order in V. In the usual procedure, known as Møller–Plesset perturbation theory (MPPT), H_0 is chosen to be the Hartree–Fock Hamiltonian and a Rayleigh–Schrödinger perturbation expression for any arbitrary order is performed to obtain the correlation energy. Although the MPPT approach is size consistent in each order, it is not convergent for all values of the model parameters and, hence, the infinite summation is usually truncated to an arbitrary order, the most commonly used procedures being the second (MP2) or fourth order (MP4) perturbation calculations. Despite the size consistency of the MPPT approach, the CI method is more commonly used to treat correlations in quantum chemistry because it is variational and conceptually simple. In the CI method the N-electron states are expanded in terms of a basis set consisting of N-electron Slater determinants. The coefficients in the expansion are determined variationally. For a given basis set of one electron orbitals the full CI solution (FCI) is obtained when the expansion includes all possible N-electron Slater determinants. The CI approach is size consistent only when all possible configurations are used—when a FCI calculation is performed. However, the FCI calculation is not feasible for extended systems because of the enormous computational resources required and, usually, the results for a series of finite systems are used to extrapolate to the infinite limit. To obtain a correct description of the properties of the extended systems it is important that the results of the finite systems are size consistent, so that a FCI calculation must be performed for at least some of the finite systems.

A full configuration interaction calculation, even with minimal basis set is impracticable for smaller systems and impossible for larger systems and one usually resorts to limited configuration interaction calculations. The MP2 perturbation method begins with the Hartree–Fock solution for the ground state and seeks to improve it through a perturbation calculation in the second order. The most widely used CI calculation also starts with the HF ground state solution (the best single Slater determinant representing the ground state), and then adds configurations in which limited number of electrons have been promoted from the occupied to the virtual HF orbitals. Singly excited (SCI) (Refs. 25–27) and singly and doubly excited (SDCI) (Refs. 20–22) approximations include all single excitations and all single and double excitations, respectively. Both the methods have been applied to estimate the NLO responses of conjugated systems, the former being successful only in estimating the first hy-

TABLE I. Number of Slater determinants (SD) and spin symmetry adapted configurations (SSAC) in a full CI calculation of polyenes up to 14 carbon atoms.

N	SD	SSAC
4	36	20
6	400	175
8	4 900	1 764
10	63 504	19 404
12	853 776	226 512
14	11 778 624	2 760 615

perpolarizability of donor–acceptor systems. While many of the *ab initio* calculations which include correlation use the MP2 (Refs. 28–30) approach, most of the semiempirical methods used to study the excited states and their properties employ the CI approach.[18–22,25–27] There are however, a few *ab initio* calculations that use either limited CI or full CI amongst all excitations outside a frozen core.[23,31] Other variants include the complete active space self-consistent-field approach and the second order perturbation theory method known as the CASPT2 approximation.[32] Whatever the order of the configuration interaction it is important to obtain a spin-symmetry adapted linear combination of the configurations so as to conserve the total spin and hence utilize the spin invariance of the Hamiltonian. This exploitation of the spin invariance reduces the cpu times and storage requirements in large scale computations and gives more easily interpreted results. Table I gives the total number of Slater determinants and the number of Spin symmetry adapted configurations in a FCI calculation for polyenes of up to 14 carbon atoms. The table clearly shows the advantage of using the spin symmetry adaptation in large scale CI calculations.

There are a number of procedures for the construction of spin symmetry adapted basis sets.[33,34] These include the explicit diagonalization of the S^2 (the total spin) operator, the Lowdin projection operator technique, the symmetry group approach, the unitary group approach and the valence bond (VB) method. Of the above methods the VB method, in its original form, is the most chemically intuitive and has been extensively used in the quantum chemical applications, especially when one writes the resonance structures of a given system. The next subsection briefly outlines a method, based on the valence bond diagrams, for generating a spin symmetry adapted basis.

A. The valence bond method for spin symmetry adaptation

For any given number of sites N, electrons N_e, and spin S one can generate all possible linearly independent valence bond diagrams $|i\rangle$, following Rumer–Pauling rules, details of which can be found elsewhere.[19,33–35] A binary representation of these diagrams leads to an efficient method of generation and storage. A configuration of N orbitals is specified by a $2N$ bit integer, associating 2 bits per orbital. The binary sequence ''11'' corresponds to a doubly occupied site and a ''00'' corresponds to an empty site, a ''10'' for a line beginning and a ''01'' for a line ending representing a covalent bond. Thus each VB diagram can be generated and stored as

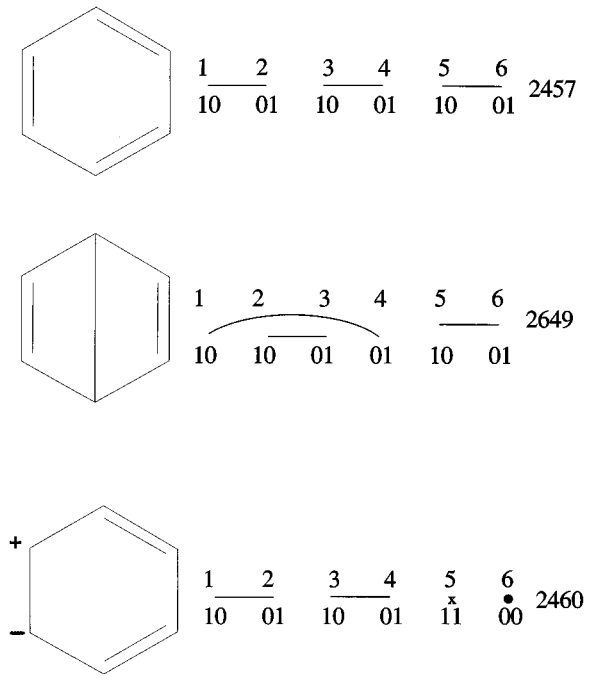

FIG. 1. Binary representation of the Kekule, Dewar, and ionic valence bond diagrams for benzene and the corresponding unique decimal integers.

a positive integer $I_k < 2^{2N}$. In order to generate the linearly independent set of VB diagrams for a given N, N_e, and S, we start with the lowest integer diagram, the integer representing the most ionic diagram having all C^- ions to the right (in the context of polyenes), and systematically shift the bits to the left and check the validity of the diagram thus formed. The bit shifting is continued until the highest integer diagram, the integer representing the other most ionic diagram, having all the C^- to the left, is obtained. The procedure is quite rapid and can be generalized to larger systems where one can make use of two integers to represent a VB diagram. For example the two Kekule structures and examples of Dewar and ionic diagrams of benzene, with their binary representation and the corresponding integers, are given in Fig. 1.

The above procedure can be extended to the generation of the spin symmetry adapted basis within the HF MO framework. Here the bit representation is exactly analogous to that previously defined for doubly occupied and unoccupied site, namely a ''11'' represents a doubly occupied MO and a ''00'' represents an empty MO. In the case of single occupancy we associate a ''10'' with an electron having α spin and a ''01'' to an electron having β spin. The generation of the basis is also analogous to the VB method; the HF MOs are arranged in order of decreasing energy and the occupancies of the MOs are represented by pairs of bits. In this representation all the occupied orbitals are on the right and the ground state is represented by this lowest integer diagram. From this integer all the other integers representing all possible spin pairing schemes, for a particular S, are generated by the shift procedure defined before. The shifting is continued until the highest integer diagram, in which all the

occupied orbitals of the HF ground state are empty and all the unoccupied orbitals are doubly occupied, is generated. In the case of larger systems we associate two integers, one representing the occupied orbitals of the HF ground state and the other representing the unoccupied MOs. To call these diagrams VB diagrams would be a misnomer since VB diagrams represent the various resonance structures of a chosen system written in terms of atomic orbitals. These diagrams will therefore be referred to as molecular orbital spin pairing (MOSP) diagrams. It is important to note that in addition to the difference in nomenclature, the MOSP and VB diagrams differ energetically. For example in the diagrammatic VB representation the lowest energy diagram would correspond to a diagram in which all the sites are covalently bonded. This however would correspond to an excited diagram in the MOSP representation. The diagram representing the HF ground state in the MOSP scheme would be identified, in the VB method, with one of the highest energy states. However some of the other properties, such as the charge orthogonality, of the VB diagrams are retained by the MOSP diagrams. The set of spin pairing diagrams generated in terms of the MOs form a nonorthogonal basis. A spin symmetry adapted orthogonal MO basis can be generated by orthogonalizing the MOSP diagrams using the Gram–Schmidt procedure. Thus assuming the $V_1,V_2,V_3,\ldots,V_n$, to be the set of configurations representing the linearly independent MOSP diagrams, the set of orthogonal spin symmetry adapted MO configurations, $M_1,M_2,M_3,\ldots,M_n$, can be generated by the Gram–Schmidt orthogonalization procedure as follows:

$$M_1=V_1, \tag{1}$$

$$M_2=V_2-\langle V_1|M_1\rangle V_1, \tag{2}$$

$$\vdots$$

$$M_n=V_n-\sum_{i=1}^{n-1}\langle V_i|M_i\rangle V_i. \tag{3}$$

Once the set of MOSP diagrams is generated, the calculation of the set of orthogonal spin symmetry adapted MO configurations is straightforward, provided the overlap matrix between the MOSP diagrams is known. It is important to note here that, it is possible to perform a CI calculation with the unorthogonalized basis by rewriting the CNDO Hamiltonian such that the integrals are transformed from the atomic orbital basis to a MO representation. Such a procedure has been used previously in FCI calculations with the PPP Hamiltonian.[18] This procedure however leads to an unsymmetric CI matrix and may not be an efficient method in limited CI calculations, where the sparseness of the CI matrix is greatly reduced, so that it has to be stored in its entirety. In the following paragraphs we briefly outline an efficient method for calculating and storing the overlap matrix S_{ij} (for further details see Ref. 33).

The order of the overlap matrix S_{ij} is the same as the number of excited state determinants and hence direct evaluation of S_{ij} is impracticable for larger bases. For example there are 19 404 singlet MOSP diagrams for a polyene of 10 carbon atoms and hence storing all the elements of the overlap matrix requires a large amount of memory even if stored as a sparse matrix. On the other hand if we exploit the charge orthogonality of the MOSP diagrams, the basis can be rearranged such that S_{ij} is block-diagonal with blocks of the same size being identical. Nonvanishing S_{ij} requires two MOSP diagrams to have an identical occupancy in each site. For example MOSP diagrams which have an occupancy of one in all the orbitals (purely covalent diagrams in the VB representation) are orthogonal to any diagram which has more than one electron in any of the sites (an ionic diagram in the VB representation), while diagrams with all the MOs doubly occupied or those in which only two MOs are singly occupied are orthogonal to all others.

The size of a given block in the overlap matrix depends on the number of linearly independent pairing schemes for a given charge distribution and the number of such blocks depends on the number of such charge distribution. For example, for $2N$ electrons in $2N$ orbitals and total spin $S=0$, the first block contains

$$P_0(2N)=\frac{(2N!)}{N!(N+1)!} \tag{4}$$

linearly independent diagrams in which all the MOs are singly occupied. This block occurs only once, since the charge distribution is unique. The next blocks have $P_0(2N-2)$ diagrams in which $(N-2)$ MOs are singly occupied, one is doubly occupied and one empty. There are $2N(2N-1)$ different charge distributions for one empty and one doubly occupied MO. The general result for $M<N$ pairs of doubly occupied and empty MOs and $N-2M$ singly occupied MOs is,

$$R(N,M)=\frac{(2N)!}{(2N-2M)!M!M!} \tag{5}$$

blocks of $P_0(2N-2M)$. Within the blocks of the same charge distribution, S_{ij} is computed using the Pauling island counting.[19] Islands are generated by superposition of diagrams. For example, for $N-M$ lines, the number of islands is $1<i<N-M$ and is the number of disconnected cycles found on superposing the two structures. Any diagram superposed on itself gives $i=N-M$. The general results for diagrams $|i\rangle$ and $|j\rangle$ with the same charge distribution and $N-M$ bonds is

$$S_{ij}=(-2)^{i-N+M}, \tag{6}$$

where i is the number of islands. Thus, by this procedure, instead of calculating a 19 404×19 404 overlap matrix for a polyene of 10 carbon atoms we need to calculate only one 42×42, one 14×14, one 5×5, and one 2×2 submatrix, reducing both the storage and computational time. Because of the block-diagonal structure of the MOSP overlap matrix the spin symmetry adapted MO basis is also generated blockwise, even though the MO basis in principle requires an expansion of all the previous MOSP diagrams, since the coefficient of a MOSP diagram belonging to a different block is zero. In Table II we list some of the singly and doubly excited configurations and their corresponding MOSP diagrams.

The method described above is quite general and can be used with any model Hamiltonian or in an *ab initio* calcula-

TABLE II. Singly and doubly excited spin-adapted configurations, the corresponding VB diagrams.

SSAC	VB diagrams
$\vert^1\psi_a^r\rangle$	$\vert x\ .\rangle$
$\vert^1\psi_{aa}^{rr}\rangle$	$\vert .\ x\ x\ .\rangle$
$\vert^1\psi_{aa}^{rs}\rangle$	$\vert .\ x$ -----$\rangle$
$\vert^1\psi_{ab}^{rr}\rangle$	$\vert$---- $x\ .\rangle$
$\vert^A\psi_{ab}^{rs}\rangle$	$\vert$----- -----$\rangle$
$\vert^B\psi_{ab}^{rs}\rangle$	$\vert$----- -----$\rangle+\vert$-----$\rangle$

tion. However, as mentioned earlier, a full configuration interaction calculation is feasible only for smaller systems even with a minimal basis set. One way to overcome this problem for calculations on larger systems is to choose an active subspace of a particular symmetry and perform a complete CI calculation within that subspace. The recent success of many of the π-electron theories such as the Pariser–Parr–Pople (PPP) models in describing the electronic and optical properties of π-conjugated systems prompts one to choose an active space formed by orbitals with π-symmetry. Furthermore previous experimental and theoretical studies have clearly demonstrated that the NLO response in these systems is largely due to the π-electrons.[7,8,19–22] In our calculation we first carry out a Hartree–Fock calculation using a variant of the CNDO/S Hamiltonian.[28] From the CNDO ground state the orbitals of π-symmetry are selected and a FCI calculation is performed within this subspace. An added advantage of working with an active space formed by π-orbitals is in reducing the cpu times in evaluating the CI matrix. The only nonzero coefficients in a MO of π-symmetry are those of the p_z atomic orbitals of the atoms in the π-framework and hence the number of terms in the summations which occur in the evaluation of the CI matrix elements is greatly reduced. For systems which lack π-symmetry it is possible to pick out an arbitrary number of occupied and unoccupied orbitals to form a window of arbitrary size around the HOMO and do a complete CI calculation. Limited CI calculation is also possible within the above scheme by restricting the maximum number of ''ones'' in the segment of the binary numbers representing the virtual MOs included in the calculation when generating the MOSP diagrams. For example if we wish to do a singly and doubly excited configuration interaction calculation for 1,3,5,7-octatetraene then we first pick out the eight π-orbitals from the Hartree–Fock ground state and limit the number of electrons in the segment formed by four unoccupied orbitals to a maximum of 2 electrons. This way one can generate configurations representing limited excitation and hence perform limited CI calculation of any desired order.

B. The correction vector method

Using the spin symmetry adapted MO basis, the corresponding CI matrix is set up and is diagonalized to obtain the corresponding eigenstates to compute the linear and nonlinear optical properties of the chosen systems. The NLO coefficients reported in this paper are the frequency dependent polarizability and the third harmonic generation (THG) coefficient. Since the MO configurations are orthogonal the resultant CI matrix is symmetric, though much less sparse than the one obtained from the valence bond method. In all cases an exact diagonalization of the CI matrix using the Davidson algorithm[36] is carried out to obtain a few low lying states and for polyenes up to eight carbon atoms a complete diagonalization, to obtain all the eigenvalues and the corresponding eigenstates, is also performed. The complete diagonalization is possible only for smaller systems and in those systems we use the eigenvalues and eigenvectors to do a sum-over-states calculation of the NLO coefficients, to identify the essential states contributing to the final value of the coefficient. For larger systems where a complete diagonalization of the CI matrix is not possible we use the correction vector method, briefly outlined below, to compute the NLO coefficients. The correction vector method and the SOS method should in principle give the same value of the NLO coefficients when the same set of basis functions are used in the CI calculation. The results for the NLO coefficients of smaller systems, which have been calculated by both the methods, verify this.

The first order correction to the ground state obeys the equation[37]

$$(H-E_G+\hbar\omega)\phi_i^{(1)}=-\mu_i\vert G\rangle, \tag{7}$$

where $\vert G\rangle$ is the ground state of the system after configuration interaction, E_G is the corresponding energy, and μ_i is the dipole displacement operator, defined as $\mu_i=\mu_i-\langle O\vert\mu_x\vert O\rangle$. Solution to Eq. (7) can be obtained by expanding the correction vector $\phi_i^{(1)}$ in terms of the same set of excited determinants describing the ground and all the excited states, which can be written as

$$\phi_x^{(1)}=\sum_i c_{ix}^{(1)}\vert\theta_i\rangle, \tag{8}$$

where θ_i's are the excited configurations. Since the correction vector and the ground state are expanded in terms of the same set of configurations, substitution of the expansions for $\vert G\rangle$ and ϕ in Eq. (7) allows the expansion coefficients $c_i^{(1)}$ for ϕ to be obtained from a set of linear inhomogeneous equations by matching coefficients. This procedure yields,

$$H(\omega)\cdot c_x(\omega)=\mu_x, \tag{9}$$

where

$$H_{ij}(\omega)=\langle\theta_i\vert H_0-E_g+\hbar\omega\vert\theta_j\rangle, \tag{10}$$

and

$$(\mu_x)_i=\langle\theta_i\vert\mu_x\vert G\rangle. \tag{11}$$

The problem has now been reduced to solving a system of linear inhomogeneous equations. Their solution is obtained for positive omegas using the Gauss–Seidel iteration procedure, since the associated matrix is positive definite. The scheme of Ramasesha[38] is used for negative omegas when the associated matrix is nondefinite. Once $\phi_x^{(1)}$ is known the frequency dependent polarizability, in atomic units, can be written in terms of the correction vector as

$$\alpha_{ij}(-\omega;\omega)=\langle G\vert\mu_i\vert\phi_j^{(1)}(\omega)\rangle+\langle G\vert\mu_i\vert\phi_j^{(1)}(-\omega)\rangle. \tag{12}$$

TABLE III. Electronic, linear, and nonlinear optical properties of butadiene.

Order of CI	$\hbar\omega$	$\Delta E(1\ ^1B_u)$	$\alpha(\omega;\omega)$ (in a.u.)			$\gamma(3\omega;\omega,\omega,\omega)$ (in 10^3 a.u.)			
			α_{xx}	α_{xy}	α_{yy}	γ_{xxxx}	γ_{xxyy}	γ_{yyxx}	γ_{yyyy}
1	0.30	5.52	64.61	26.31	13.32	−0.963	−0.459	−0.448	−0.099
	0.65		65.32	26.59	13.44	−1.030	−0.516	−0.498	−0.110
	1.17		67.43	27.43	13.80	−1.303	−0.782	−0.726	−0.159
2	0.30	5.83	43.36	16.54	8.84	0.643	0.061	0.065	0.018
	0.65		43.78	16.70	8.90	0.738	0.070	0.072	0.020
	1.17		45.04	17.16	9.10	1.168	0.111	0.096	0.030
3	0.30	5.78	44.16	17.05	9.21	0.527	0.019	0.024	0.004
	0.65		44.61	17.22	9.28	0.610	0.024	0.027	0.005
	1.17		45.92	17.72	9.50	0.990	0.047	0.037	0.009
4	0.30	5.80	43.75	16.86	9.11	0.558	0.028	0.032	0.006
	0.65		44.19	17.03	9.17	0.644	0.033	0.036	0.007
	1.17		45.49	17.51	9.38	1.040	0.060	0.050	0.013

The second order correction to $|G\rangle$ satisfies the linear equation

$$(H_0-E_g+\hbar\omega)\phi_{xy}^{(2)}(\omega_1,\omega_2)=-\mu_y\phi_x^{(1)}(\omega_1). \tag{13}$$

The method of solving for $\phi_{xy}^{(2)}$ is entirely analogous to the method of solving for $\phi_x^{(1)}$. The second order correction vector $\phi_{xy}^{(2)}$ is also expanded in terms of θ and the coefficients $c_{xyi}^{(1)}(\omega_1;\omega_2)$ are obtained from the linear equations

$$H(\omega_2)\cdot c_{xy}(\omega_1,\omega_2)=\mu_{xy}(\omega_1), \tag{14}$$

where

$$H_{ij}(\omega_2)=\langle\theta_i|H_0-E_g+\hbar\omega_2|\theta_j\rangle, \tag{15}$$

and

$$(\mu_{xy})_i(\omega_1)=\langle\theta_i|\mu_y|\phi_x^{(1)}(\omega_1)\rangle. \tag{16}$$

Since $\phi_{xy}^{(2)}$ is sufficient for the evaluation of NLO coefficients up to fourth order [$\chi^{(4)}$] contributions from $\phi^{(3)}$ and higher order corrections are not of immediate interest, although generalization to higher order is fairly simple. The dominant component of the THG coefficient $\gamma_{xxxx}(-3\omega;\omega,\omega,\omega)$, in atomic units, can now be written in terms of $\phi_x^{(1)}$ and $\phi_{xy}^{(2)}$ as follows:

$$\begin{aligned}\gamma_{xxxx}(-3\omega;\omega,\omega,\omega)&=(8)^{-1}[\langle\phi_x^{(1)}(-3\omega)|\mu_x|\phi_{xx}^{(2)}(-2\omega;-\omega)\rangle\\&\quad+\langle\phi_{xx}^{(2)}(2\omega;\omega)|\mu_x|\phi_x^{(1)}(-\omega)\rangle+\omega\rightarrow-\omega],\end{aligned} \tag{17}$$

where $\omega\rightarrow-\omega$ indicates the same matrix elements with new arguments.

III. RESULTS AND DISCUSSION

All the molecules studied in this paper are planar and the coordinate system has been chosen so that they lie in the $x-y$ plane with the x-axis directed along the chain backbone. The dominant components of the linear polarizability are α_{xx}, α_{xy}, and α_{yy} while γ_{xxxx}, γ_{xxyy}, and γ_{yyyy} are the largest THG coefficients. The NLO properties reported are essentially those of the π-framework as extracted from the ground state of a CNDO calculation. Standard planar geometries were used; for the *trans* polyenes, r(C═C)=1.340 Å, r(C–C)=1.46 Å, r(C–H)=1.08 Å, and all bond angles 120°; for benzene, r(C–C)=1.397 Å, r(C–H)=1.08 Å, and all bond angles 120°.

In Tables III, V, VIII, X, and XI, respectively we present results of our calculations on the electronic and optical properties of butadiene, hexatriene, benzene, octatetraene, and longer polyenes up to 16 carbon atoms. The tables include the values of the excitation energy of the lowest dipole allowed (^1B_u) state and the dominant components of the frequency dependent polarizability and THG hyperpolarizability at three different excitation frequencies. All the data are examined as a function of the increasing order of CI used in the calculation. The order of CI is specified by the integer n, defined such that all configurations in which n or fewer electrons are excited are included in the calculation (n=1, SCI; n=2, SDCI etc.). In Tables IV, VII, and IX we present the π-electron bond orders and charge densities in three salient states of butadiene, hexatriene, and benzene respectively, as a function of n. In the following paragraphs the results for individual molecules are discussed.

A. *Trans*-1,3-butadiene

It can be seen from Table III that, as expected, the correct sign of the THG coefficient is obtained only when correlations at the level of SDCI are included. The larger value of the SCI polarizability is attributable to the smaller SCI one photon excitation energy. Inclusion of configurations with $n>2$ has a negligible effect. This is to be expected as higher excitations are not of much importance in a small system such as butadiene. Our value of the one photon excitation energy from the FCI calculation, 5.80 eV, is in very good agreement with the experimental value of 5.92 eV.[40,41] The relative location of the one photon $1\ ^1B_u$ and the two photon $2\ ^1A_g$ state has been one of the major issues in the electronic spectrum of butadiene.[42,43] There are reported experimental values of the two photon state ranging from 5.4 to 7.3. Recent *ab initio* CASSF, CASPT2 calculations place the two photon $2\ ^1A_g$ state at 6.27 eV which is about 0.05 eV above the lowest dipole allowed $1\ ^1B_u$ state.[44] However, a number of semiempirical calculations that include correlations at the level of SDCI find that the two photon $2\ ^1A_g$ state lies below the one photon $1\ ^1B_u$ state.[19–22] A recent result

TABLE IV. Calculated π-bond orders for the unique bonds and π-charge densities of unique carbon atoms of the three important π-electron states of butadiene as a function of the order of CI.

		Bond order		Charge density	
Order of CI	Symmetry	C_1–C_2	C_2–C_3	C_2	C_2
1	$G(1\ ^1A_g)$	0.957	0.289	−0.023	0.023
	$1\ ^1B_u$	0.478	0.620	−0.152	0.152
	$2\ ^1A_g$	0.475	0.156	−0.015	0.015
2	$G(1\ ^1A_g)$	0.912	0.304	−0.020	0.020
	$1\ ^1B_u$	0.497	0.541	−0.012	0.012
	$4\ ^1A_g$	0.266	0.354	0.038	−0.038
3	$G(1\ ^1A_g)$	0.912	0.304	−0.020	0.020
	$1\ ^1B_u$	0.491	0.538	−0.012	0.012
	$4\ ^1A_g$	0.252	0.374	0.030	−0.030
4	$G(1\ ^1A_g)$	0.912	0.304	−0.020	0.020
	$1\ ^1B_u$	0.491	0.538	−0.012	0.012
	$4\ ^1A_g$	0.230	0.392	0.038	−0.038

from resonance Raman scattering experiment places the $2\ ^1A_g$ state at 5.87 eV which is 0.05 eV lower than the $1\ ^1B_u$ state.[44] The two photon excitation energy from our FCI calculation is 5.63 eV and is in good agreement with the latter experimental value.

The good agreement between the absolute values of the calculated and experimental optical gap ($1\ ^1A_g$–$1\ ^1B_u$) is mainly a consequence of the success of the parametrization scheme used since the $1\ ^1B_u$ state in butadiene is not greatly affected by CI.

The charge densities and bond orders for butadiene are shown in Table IV for the states which make the most significant contributions to the hyperpolarizability. The results for the SCI case differ from the others and the calculated hyperpolarizability for $n=1$ is negative. For all other cases a similar pattern of significant states appears. The lowest dipole allowed transition from the ground state, $1\ ^1A_g \rightarrow 1\ ^1B_u$, and the transition $1\ ^1B_u \rightarrow 4\ ^1A_g$, to one of the higher two photon allowed states, have substantial transition moments (5.82 and 8.55 D, respectively, for $n=4$) which couple these excited states into the perturbation theory expansion for the hyperpolarizability. Table IV shows that, for the $4\ ^1A_g$ state, there is a large difference in the charge densities on the two nonequivalent carbons, a feature which is associated with an enhancement of the transition moment for $1\ ^1B_u \rightarrow 4\ ^1A_g$. The contribution of this transition to the THG coefficient compensates the initial negative bias from the first transition and hence produces a net positive value for the THG coefficient.

B. *Trans*-1,3,5-hexatriene

Again we see that configurations at least at the level of double excitations are necessary to obtain the correct sign of the THG coefficient and the SCI calculation overestimates the polarizability. Unlike the case of butadiene, where a SDCI calculation reproduces most of the electronic and optical properties, the hexatriene results are more sensitive to correlation effects and configurations of higher order affect the electronic and optical properties. For example the change in the electronic and optical properties of hexatriene in going from a CI of order 2 to 3 is much more pronounced than in the case of butadiene. There is no appreciable further change in the properties obtained from CI calculations of order greater than 3. In Fig. 2 we present a plot of the evolution of the THG hyperpolarizability of hexatriene at an excitation frequency if 1.17 eV as a function of the number of states added into the SOS expression for different orders of CI. It can be seen from the plot that the qualitative nature of the evolution of the THG coefficient from all CI calculations of order greater than 2 is similar. The first major contribution, which is negative, comes from the 3rd state, the dipole allowed ^1B_u state. The second contribution comes from the 8th state, a ^1A_g state, in combination with ^1B_u, and is positive. The contributions from higher states are minimal and hence the summation is stopped at 50 states. The difference between the model exact (FCI) value of the THG coefficient and that from CI of different orders is also noteworthy. Although the SDCI calculation reproduces the qualitative nature of the evolution obtained from a FCI calculation, it slightly overestimates the coefficient, as each state is added into the SOS expression. This however does not happen in

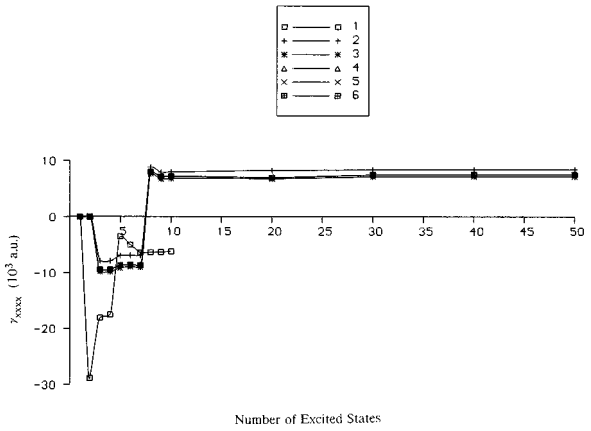

FIG. 2. The variation of the dominant component of the THG hyperpolarizability γ_{xxxx} $(3\omega;\omega,\omega,\omega)$ at an excitation energy of 1.17 eV for hexatriene as excited states of increasing energy are added into the SOS expansion. The six plots represent the six calculations carried out for each order of CI calculation, specified by an integer (see text).

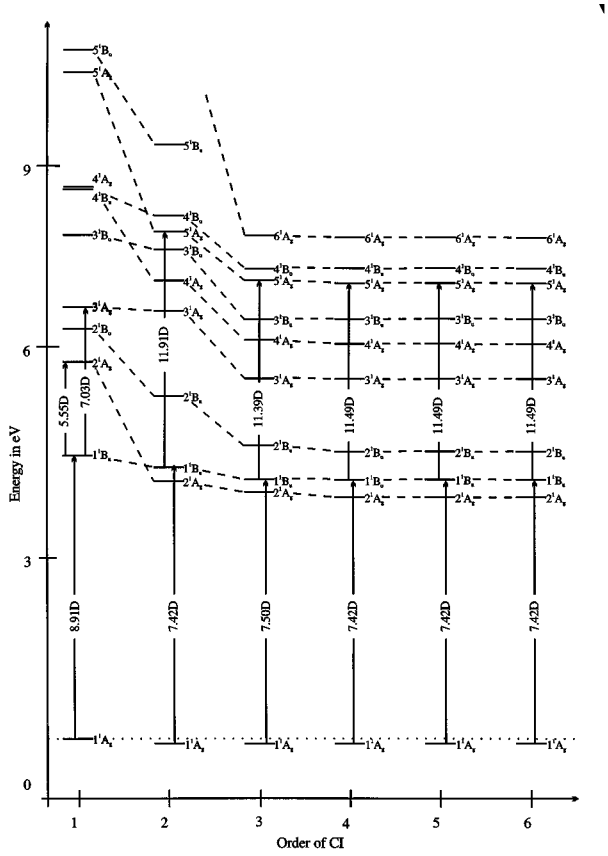

FIG. 3. Ten low lying states of hexatriene plotted as a function of the order of the CI calculation. The symmetry labeling of each of the state are also given. The order of the CI is specified by an integer (see text for details).

CI calculations of order greater than 2, where the curves coincide. The qualitative nature of the evolution of the THG coefficient for CI of order 1 is as usual totally different from the others.

A better understanding of the evolution pattern can be obtained when one looks at the nature of first ten low lying states, beyond which there seems to no qualitative or quantitative change in the value of the THG coefficient. In Fig. 3 we present the first ten low lying states as obtained from CI calculations of different order. The figure also gives the transition moments between the states making major contributions to the THG coefficient, namely $\mu(1\ ^1A_g \rightarrow 1\ ^1B_u)$ and $\mu(1\ ^1B_u \rightarrow 5\ ^1A_g)$ when $n \geqslant 2$ and $\mu(1\ ^1A_g \rightarrow 1\ ^1B_u)$, $\mu(1\ ^1B_u \rightarrow 2\ ^1A_g)$ and $\mu(1\ ^1B_u \rightarrow 3\ ^1A_g)$ for SCI. The figure brings out clearly the importance of correlation on the relative positions of the states. Even in the case of hexatriene the actual ordering of the states is still a subject of controversy. While many *ab initio* calculations, including recent CASSF and CASPT2 studies,[44] place the $2\ ^1A_g$ state above the one photon $1\ ^1B_u$ state,[45,46] semiempirical calculations, which include more electron correlation, reverse this order.[19–22] A recent two-photon absorption study of hexatriene finds a two photon allowed band with a maximum at 5.21 eV which is 0.16 eV above the dipole allowed state.[47] Although the exact position of the $2\ ^1A_g$ state is a matter of much controversy the $1\ ^1B_u$ state of hexatriene has been well characterized experimentally both by vacuum UV spectroscopy, absorption spectroscopy of jet cooled molecules and electron impact. The energy corresponding to the peak for this transition occurs at 4.95 eV and has been taken as the vertical transition energy. The excitation energies of the $1\ ^1B_u$ and $2\ ^1A_g$ states from our FCI calculation are 5.01 and 4.71 eV, respectively. Our value of 5.01 eV for the $1\ ^1A_g \rightarrow 1\ ^1B_u$ transition is in very good agreement with both the experimental value of 4.95 eV and the *ab initio* calculated value of 5.01 eV. The excitation energy of the $2\ ^1A_g$ state is in better agreement with the earlier experimental finding that places the $2\ ^1A_g$ state at 4.40 eV.[48] The ordering of the states from SCI calculation is different from the ordering of the states obtained from CI calculations of higher order, and, while the SDCI

TABLE V. Electronic, linear, and nonlinear optical properties of hexatriene.

Order of CI	$\hbar\omega$	$\Delta E(1\ ^1B_u)$	f	$\alpha(\omega;\omega)$ (in a.u.)			$\gamma(3\omega;\omega,\omega,\omega)$ (in 10^3 a.u.)			
				α_{xx}	α_{xy}	α_{yy}	γ_{xxxx}	γ_{xxyy}	γ_{yyxx}	γ_{yyyy}
1	0.30	4.70		131.22	44.87	20.96	−4.048	−1.617	−1.554	−0.272
	0.65			133.21	45.53	21.20	−4.416	−1.907	−1.797	−0.311
	1.17			139.24	47.51	21.92	−6.210	−3.710	−3.248	−0.549
2	0.30	5.14		85.86	26.61	13.37	3.756	0.235	0.260	0.053
	0.65			86.94	26.92	13.48	4.482	0.278	0.286	0.060
	1.17			90.17	27.87	13.82	8.428	0.505	0.410	0.097
3	0.30	4.99		90.48	28.56	14.58	2.858	0.030	0.057	0.003
	0.65			91.69	28.92	14.71	3.490	0.046	0.063	0.006
	1.17			95.32	30.01	15.11	7.157	0.146	0.075	0.020
4	0.30	5.00		88.29	27.67	14.19	3.082	0.090	0.116	0.015
	0.65			89.46	28.02	14.31	3.740	0.117	0.130	0.019
	1.17			92.98	29.07	14.69	7.516	0.273	0.186	0.041
5	0.30	5.00		88.31	27.67	14.20	3.074	0.088	0.114	0.014
	0.65			89.49	28.04	14.33	3.732	0.114	0.128	0.018
	1.17			93.00	29.08	14.70	7.502	0.268	0.182	0.039
6	0.30	5.01		88.30	27.68	14.20	3.076	0.088	0.114	0.014
	0.65			89.47	28.03	14.32	3.734	0.115	0.128	0.018
	1.17			92.98	29.07	14.69	7.506	0.269	0.183	0.039

TABLE VI. Calculated percentage contribution of the various excited configurations to the 10 low-lying electronic states of hexatriene.

State symmetry	N-tuply excited configurations						
	0	1	2	3	4	5	6
$1\ ^1A_g$	92.83	0.02	7.01	0.02	0.12	0.0	0.0
$2\ ^1A_g$	0.89	41.29	54.67	2.60	0.53	0.0	0.0
$1\ ^1B_u$	0.0	95.56	3.12	1.29	0.03	0.0	0.0
$2\ ^1B_u$	0.0	53.21	44.75	1.38	0.65	0.0	0.0
$3\ ^1A_g$	0.19	87.78	7.98	3.90	0.13	0.01	0.0
$4\ ^1A_g$	0.19	19.33	75.97	3.75	0.75	0.0	0.0
$3\ ^1B_u$	0.0	80.33	15.44	4.01	0.18	0.03	0.0
$5\ ^1A_g$	1.93	44.75	51.50	0.84	0.98	0.0	0.0
$4\ ^1B_u$	0.0	74.94	21.83	2.13	0.09	0.01	0.0
$6\ ^1A_g$	0.12	80.53	15.38	3.67	0.28	0.02	0.0

calculation reproduces the ordering of many of the low lying excited states, it overestimates their energies. The most important qualitative change observed when going from a SDCI calculation to a CI calculation of order 3 relates to the $5\ ^1B_u$ and $6\ ^1A_g$ (not shown in the figure) states. The SDCI calculation places $5\ ^1B_u$ state below $6\ ^1A_g$, whereas this order is reversed in the model exact (FCI) calculation and for all cases where $n \geqslant 3$. As can be seen from the evolution of the THG coefficient and from Table V, there seems to be little qualitative or quantitative change beyond $n=3$. The CI calculation of order 3 reproduces the correct ordering and the position of the states in the electronic spectrum of hexatriene. The percentage contribution of the various excited configurations to the first ten low lying excited states of hexatriene is shown in Table VI. It can be seen from the table that the contributions of quadruply and higher excited configurations to these states are minimal. The ground state as expected is largely accounted for by the HF solution with a small contribution from the doubly excited configurations. The first dipole allowed, $1\ ^1B_u$, excited state is dominated by singly excited configurations with small contributions from doubly and triply excited configurations. The $2\ ^1A_g$ and $5\ ^1A_g$ states contain nearly equal admixtures of singly and doubly excited configurations, while $3\ ^1A_g$ is mainly a superposition of a number of singly excited configurations and the $4\ ^1A_g$ of doubly excited configurations. The doubly excited component of the $5\ ^1A_g$ state consists almost entirely of the configuration in which two electrons have been excited from the HOMO to the LUMO. It is therefore very strongly coupled via the dipole operator to the $1\ ^1B_u$ state and makes a major positive contribution to third order nonlinear effects through combinations of matrix elements which link the ground state, $1\ ^1B_u$ and $5\ ^1A_g$. It is also interesting to note that although the $3\ ^1A_g$ and $4\ ^1A_g$ states lie below the $5\ ^1A_g$ state the transition moment $1\ ^1B_u \rightarrow n\ ^1A_g$ for the former two states is much less than for the latter.

Another important feature to emerge from the plot is a possible reason for the change in sign of the THG coefficient obtained from different CI calculations. The first allowed transition, the $1\ ^1A_g \rightarrow 1\ ^1B_u$ transition, has a large transition moment in the SCI calculation and hence the contribution from this transition is a large negative value, about 30 000 a.u. The lowest two photon transitions (in the case of the SCI calculation there are two transition of similar intensities, the $1\ ^1B_u \rightarrow 2\ ^1A_g$ and $1\ ^1B_u \rightarrow 3\ ^1A_g$) have a relatively small value of the transition dipole moment. These transitions in combination with the first give a positive contribution to THG coefficient. However as the value of this contribution is relatively small, about 25 000 a.u., compared to the initial negative bias the final value of the THG coefficient remains negative. On the contrary the initial negative bias from the other calculations are small, about 10 000 a.u., as the first transition has a relatively smaller transition moment. The second contribution is a large positive one, about 20 000 a.u., which comes from a large transition moment of the two photon transition. This appears to be the reason for the change in sign of the THG coefficient obtained from CI calculations of order greater than 2. Support for this conjecture comes the results of the charge densities and bond order calculations (Table VII). It can be seen that while there is a large charge transfer in the second transition ($1\ ^1B_u \rightarrow 5\ ^1A_g$), the charge transfer in the first transition ($1\ ^1A_g \rightarrow 1\ ^1B_u$) is small. Although the THG coefficients obtained from CI calculations of order greater than or equal 2 remain positive, there is a change in magnitude. This can be attributed to the change in the magnitude of both the transition moments and the excitation energies of the relevant states when going from a SDCI calculation to a CI calculation of order 3. However CI calculations of order greater than 3 does not seem to affect the properties much and hence the THG coefficient remains relatively stabilized.

C. Benzene

The electronic, linear, and nonlinear optical properties of benzene as a function of the order of CI are given in Table VIII. Most of the arguments presented in the previous paragraph hold good, but for benzene it is necessary to increase the order of CI excitation to $n=4$ before consistent results for the THG coefficients are obtained, even though the excitation energies of the dipole allowed state from the $n=3$ and $n=4$ calculations are in good agreement. The evolution of the THG hyperpolarizability as states of higher energy are added into the SOS expression and the electronic spectrum of benzene as a function of the order of CI are presented in Fig. 4. Figure 4 clearly shows the importance of the higher states in determining the sign of the THG coefficient in benzene. While a major part of the final value of the THG co-

TABLE VII. Calculated π-bond orders for the unique bonds and π-charge densities of unique carbon atoms of the three important π-electron states of hexatriene as a function of the order of CI.

Order of CI	Symmetry	Bond order			Charge density		
		C_1–C_2	C_2–C_3	C_3–C_4	C_1	C_2	C_3
1	$G(1\ ^1A_g)$	0.952	0.302	0.911	−0.024	0.022	0.002
	$1\ ^1B_u$	0.702	0.542	0.474	−0.012	0.019	−0.007
	$3\ ^1A_g$	0.609	0.338	0.671	0.006	0.187	−0.193
2	$G(1\ ^1A_g)$	0.909	0.317	0.863	−0.021	0.019	0.002
	$1\ ^1B_u$	0.704	0.514	0.483	−0.017	0.027	−0.010
	$5\ ^1A_g$	0.592	0.497	0.230	0.014	0.040	−0.054
3	$G(1\ ^1A_g)$	0.909	0.318	0.862	−0.021	0.019	0.002
	$1\ ^1B_u$	0.698	0.508	0.471	−0.014	0.030	−0.016
	$5\ ^1A_g$	0.592	0.501	0.200	0.010	0.022	−0.032
4	$G(1\ ^1A_g)$	0.904	0.319	0.858	−0.021	0.019	0.002
	$1\ ^1B_u$	0.698	0.507	0.469	−0.015	0.032	−0.017
	$5\ ^1A_g$	0.581	0.495	0.211	0.020	0.024	−0.044
5	$G(1\ ^1A_g)$	0.904	0.319	0.858	−0.021	0.019	0.002
	$1\ ^1B_u$	0.698	0.507	0.469	−0.015	0.032	−0.017
	$5\ ^1A_g$	0.581	0.495	0.211	0.020	0.024	−0.044
6	$G(1\ ^1A_g)$	0.904	0.319	0.858	−0.021	0.019	0.002
	$1\ ^1B_u$	0.698	0.507	0.469	−0.015	0.032	−0.017
	$5\ ^1A_g$	0.581	0.495	0.211	0.020	0.024	−0.044

efficient of hexatriene was obtained from the first the 10 low lying excited states, still higher states are essential to obtain the final value of the THG coefficient in benzene. This result is almost certainly a consequence of the occurrence of numerous degenerate states in the electronic spectrum of benzene. The major transitions contributing to the final value of the THG coefficient of benzene are between $1\ ^1A_{1g}$, $1\ ^1E_{1u}$, and the $5\ ^1E_{2g}$ states. Figure 4 also shows the important qualitative difference that arises from CI calculations of order greater than 2. While the large positive contribution to the THG coefficient from the SDCI calculation comes when the 23rd and 24th ($5\ ^1E_{2g}$) states are added, this positive contribution in the higher order CI calculations comes from the 21 and 22 states, which are the degenerate $5\ ^1E_{2g}$ state. This means that the $5\ ^1E_{2g}$ state descends below the $4\ ^1A_{1g}$ state in higher order CI calculations. However the positive contribution from the 21st and 22nd states in CI calculation of order greater than 2 does not results in a net positive value of the THG hyperpolarizability, which becomes positive only when the $5\ ^1A_{1g}$ (31st) state is added and this is an important qualitative difference in the evolution pattern of the THG hyperpolarizability of benzene. The excitation energy of the $1\ ^1A_{1g} \rightarrow 1\ ^1E_{1u}$ transition (6.66 eV) from the FCI calculation is in very good agreement with the experimental value of 6.90 eV (Ref. 48) and also the *ab initio* CASPT2 value of 6.52 eV.[44] The bond orders and charge densities in the three significant states of benzene are presented in Table IX. We find that there is a large charge transfer in the

TABLE VIII. Electronic, linear, and nonlinear optical properties of benzene.

Order of CI	$\hbar\omega$	$\Delta E(1\ ^1E_{1u})$	f	$\alpha(\omega;\omega)$ (in a.u.)			$\gamma(3\omega;\omega,\omega,\omega)$ (in 10^3 a.u.)			
				α_{xx}	α_{xy}	α_{yy}	γ_{xxxx}	γ_{xxyy}	γ_{yyxx}	γ_{yyyy}
1	0.30	7.77		53.57	0.0	53.57	−0.859	−0.286	−0.286	−0.859
	0.65			53.93	0.0	53.93	−0.910	−0.303	−0.303	−0.910
	1.17			54.97	0.0	54.97	−1.098	−0.366	−0.366	−1.098
2	0.30	7.03		35.08	0.0	35.08	0.234	0.078	0.078	0.234
	0.65			35.32	0.0	35.32	0.253	0.084	0.084	0.253
	1.17			36.00	0.0	36.00	0.326	0.109	0.109	0.326
3	0.30	6.67		38.31	0.0	38.31	0.083	0.028	0.028	0.083
	0.65			38.60	0.0	38.60	0.094	0.032	0.032	0.094
	1.17			39.44	0.0	39.44	0.141	0.047	0.047	0.141
4	0.30	6.66		37.62	0.0	37.62	0.119	0.040	0.040	0.119
	0.65			37.90	0.0	37.90	0.134	0.044	0.044	0.134
	1.17			38.73	0.0	38.73	0.194	0.064	0.064	0.194
5	0.30	6.66		37.62	0.0	37.62	0.118	0.039	0.039	0.118
	0.65			37.91	0.0	37.91	0.133	0.044	0.044	0.133
	1.17			38.74	0.0	38.74	0.196	0.064	0.064	0.196
6	0.30	6.66		37.62	0.0	37.62	0.118	0.039	0.039	0.118
	0.65			37.90	0.0	37.90	0.133	0.044	0.044	0.133
	1.17			38.74	0.0	38.74	0.193	0.064	0.064	0.193

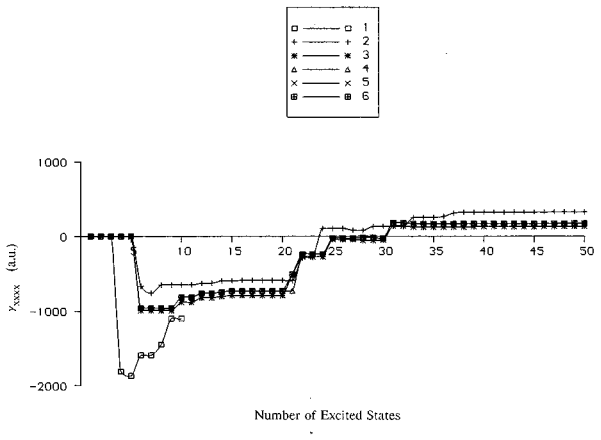

FIG. 4. The evolution pattern of the THG hyperpolarizability of benzene at 1.17 eV; for description see Fig. 2.

$1\ ^1E_{1u} \rightarrow 5\ ^1E_{2g}$ transition compared to the first allowed $1\ ^1A_{1g} \rightarrow 1\ ^1E_{1u}$ transition. The table also shows the significant change in the charge densities and bond orders of these states when the order of the CI is increased. While both the charge density and bond order of the $1\ ^1A_g$ and $1\ ^1B_u$ states from the SDCI calculation are not much different from the FCI value, the bond order and the charge densities of the $5\ ^1E_{2g}$ state vary significantly.

D. *Trans*-1,3,5,7-octatetraene

The trend exhibited (see Table X) is similar to that obtained in the case of hexatriene. The ordering of the states in the case of octatetraene is not so controversial as hexatriene or butadiene. The experimental values of the $2\ ^1A_g$ and $1\ ^1B_u$ states are 3.97 and 4.41 eV, respectively.[11] Many of the semiempirical calculations with SDCI reproduce this ordering correctly, though the exact values are different. Recent *ab initio* CASSF CASPT2 calculation also find the same ordering with the $2\ ^1A_g$ state at 4.38 and the $1\ ^1B_u$ state at 4.42 eV.[49] Our values, from the FCI calculation, of 4.10 eV ($2\ ^1A_g$) and 4.52 eV ($1\ ^1B_u$), are in very good agreement with the experimental and *ab initio* calculations. The SCI calculation fails to give the correct ordering of the states and the sign of the THG coefficient. The polarizability values obtained from the SCI calculations are larger than those obtained from other calculations, which could, even in this case be identified with a smaller optical gap of the first dipole allowed transition. The optical gap, frequency dependent polarizability and the THG coefficient seem to be stable only when CI calculation of order greater than or equal to 4 is carried out. The evolution pattern (Fig. 5) is also similar qualitatively to that obtained in the case of hexatriene.

One feature to emerge from the analysis of the electronic and optical properties of these finite polyene systems is that in all the cases a correct description of the electronic spectrum and a correct magnitude of the NLO coefficient is obtained only when a CI calculation of order greater than or equal to $N/2$, where N is the number of π-orbitals, is performed. Thus while for butadiene a SDCI calculation gives a reasonably good description of the electronic states and the NLO coefficient, CI of order 4 is essential to give a proper description of octatetraene. This is in contrast to the previous studies, where it has been generally accepted that correlations at the level of SDCI are sufficient to model polyenic systems up to eight carbon atoms.[20–22] Thus we conclude that, although the more commonly used SDCI calculation reproduces many of the qualitative features of the electronic and optical properties of conjugated systems with less than eight carbon atoms, configurations of higher order have to included in order to obtain reliable values of these properties

TABLE IX. Calculated π-bond orders for the unique bonds and π-charge densities of unique carbon atoms of the three important π-electron states of benzene as a function of the order of CI.

		Bond order			Charge density		
Order of CI	Symmetry	C_1–C_2	C_2–C_3	C_3–C_4	C_1	C_2	C_3
1	$G(1\ ^1A_g)$	0.667	0.667	0.667	0.000	0.000	0.000
	$1\ ^1E_{1u}$	0.500	0.500	0.500	0.000	0.000	0.000
	$1\ ^1E_{1u}$	0.500	0.500	0.500	0.000	0.000	0.000
	$2\ ^1E_{2g}$	0.418	0.271	0.560	0.132	−0.130	−0.002
	$2\ ^1E_{2g}$	0.415	0.562	0.273	−0.132	0.130	0.002
2	$G(1\ ^1A_{1g})$	0.647	0.647	0.647	0.000	0.000	0.000
	$1\ ^1E_{1u}$	0.455	0.421	0.564	0.011	−0.016	0.005
	$1\ ^1E_{1u}$	0.505	0.539	0.396	−0.011	0.016	−0.005
	$2\ ^1E_{2g}$	0.403	0.171	0.377	0.096	−0.040	−0.056
	$2\ ^1E_{2g}$	0.231	0.463	0.257	−0.096	0.040	0.056
3	$G(1\ ^1A_g)$	0.647	0.647	0.647	0.000	0.000	0.000
	$1\ ^1E_{1u}$	0.512	0.404	0.508	0.012	−0.006	−0.006
	$1\ ^1E_{1u}$	0.437	0.545	0.442	−0.012	0.006	0.006
	$2\ ^1E_{2g}$	0.336	0.209	0.408	0.044	−0.037	−0.007
	$2\ ^1E_{2g}$	0.299	0.426	0.228	−0.044	0.037	0.007
6	$G(1\ ^1A_g)$	0.645	0.645	0.645	0.000	0.000	0.000
	$1\ ^1E_{1u}$	0.454	0.420	0.543	0.010	−0.013	0.003
	$1\ ^1E_{1u}$	0.491	0.525	0.402	−0.010	0.013	−0.003
	$2\ ^1E_{2g}$	0.334	0.203	0.392	0.043	−0.033	−0.010
	$2\ ^1E_{2g}$	0.286	0.416	0.228	−0.043	0.033	0.010

TABLE X. Electronic, linear, and nonlinear optical properties of octatetraene.

Order of CI	$\hbar\omega$	$\Delta E(1\ ^1B_u)$	$\alpha(\omega;\omega)$ (in a.u.)			$\gamma(3\omega;\omega,\omega,\omega)$ (in 10^4 a.u.)			
			α_{xx}	α_{xy}	α_{yy}	γ_{xxxx}	γ_{xxyy}	γ_{yyxx}	γ_{yyyy}
1	0.30	4.18	213.22	65.70	29.01	−1.310	−0.397	−0.377	−0.056
	0.65		217.30	66.91	29.40	−1.493	−0.491	−0.455	−0.067
	1.17		229.86	70.61	30.60	−2.851	−1.356	−1.129	−0.159
2	0.30	4.77	135.86	37.23	17.80	1.191	0.056	0.062	0.011
	0.65		137.83	37.73	17.96	1.467	0.068	0.070	0.012
	1.17		143.79	39.25	18.44	3.223	0.139	0.110	0.021
3	0.30	4.48	150.17	42.01	20.38	0.904	−0.002	0.006	−0.001
	0.65		152.64	42.65	20.58	1.167	0.0001	0.006	−0.0001
	1.17		160.16	44.62	22.21	3.191	0.024	−0.002	0.002
4	0.30	4.52	143.84	39.64	19.46	0.985	0.020	0.028	0.003
	0.65		146.18	40.25	19.65	1.257	0.028	0.032	0.004
	1.17		153.26	42.07	20.24	3.271	0.087	0.049	0.10
5	0.30	4.52	144.02	39.73	19.53	0.978	0.018	0.026	0.003
	0.65		146.20	40.27	19.68	1.248	0.029	0.031	0.004
	1.17		153.46	42.17	20.31	3.256	0.083	0.045	0.010
6	0.65	4.52	146.23	40.29	19.70	1.250	0.027	0.031	0.003
	1.17		153.32	42.12	20.28	3.261	0.085	0.046	0.010
8	0.65	4.52	146.23	40.29	19.70	1.250	0.027	0.031	0.003
	1.17		153.32	42.12	20.28	3.261	0.085	0.046	0.010

that are comparable to the experimental values.

E. Electronic and optical properties of longer polyenes

In Table XI we summarize the results of SDCI calculations on polyenes with 10, 12, 14, and 16 carbon atoms. An attempt at a FCI calculation for decapentaene could not be completed because the CI matrix was found to be insufficiently sparse to allow it to be stored. CI calculations for $n \leqslant 4$ were possible in this case and the results are also included in the table. It can be seen that the SDCI calculation produces positive values of the THG coefficients of these systems as expected. The quantitative differences between the CI calculations for decapentaene on increasing the order from 2 to 3 are noteworthy; the excitation energy of the $1\ ^1B_u$ state changes from 4.58 to 4.14 eV, and that of $2\ ^1A_g$ from 4.48 to 3.98 eV. On going to the case $n=4$ there is little further change in $1\ ^1B_u$ (4.20 eV) but the energy of the $2\ ^1A_g$ state is reduced to 3.76 eV. Experimental values for these states are, respectively, 4.02 and 3.10 eV.[11] Although the sign of the dominant component of the THG coefficient obtained from CI calculation of order greater or equal to 2 remains positive, variations in the magnitude and sign of the other components are seen when the order of the CI calculation is increased, as has been seen in smaller finite polyenes. One feature to emerge from the table is that the excitation energy of the allowed transition in the longer polyenes does not change much with the chain length. This is to be expected as the optical gap of an infinite polyene is known to attain a limiting value. The $1\ ^1B_u$ state is found to be the lowest singlet excited state in polyenes larger than 14 carbon atoms. This might be because correlations included at the SDCI level are not sufficient to reproduce the correct ordering in these systems.

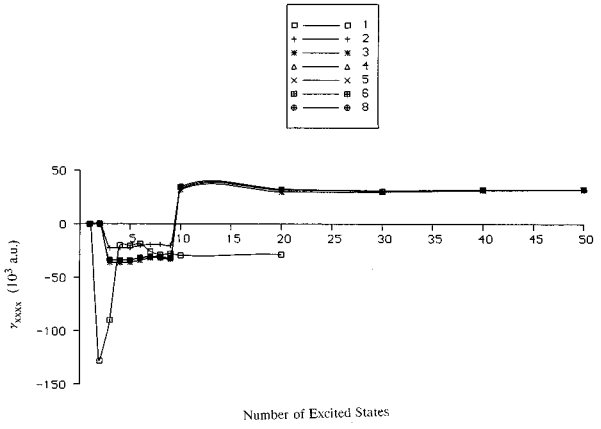

FIG. 5. The evolution pattern of the THG hyperpolarizability of octatetraene at 1.17 eV; for description see Fig. 2.

The length dependence of the dominant component of the THG coefficient, γ_{xxxx}, from SDCI and FCI calculations is presented in Fig. 6 for polyenes with 4 to 16 and 4 to 8 carbon atoms, respectively. It can be seen that the results from both the calculations obey a power law of the type $\gamma_{xxxx}=aL_x^b$. The exponent from the log–log plot of the SDCI calculation is 3.23 and that from the FCI calculation is 3.46. The good agreement is, at least partly, due to the fact that the FCI calculation has been performed only on the smaller molecules where SDCI and FCI results are expected to be similar. Our values of the exponents are also found to be good agreement with the exponents found from other calculations [3.29 from INDO/SDCI (Ref. 22) and 3.8 from DVB/FCI calculations[19]].

IV. CONCLUSION

We have described a πCI method of performing CI calculations of any order for studying the electronic and optical properties of conjugated systems within the CNDO approximation. The method uses the concepts and properties of the

TABLE XI. Electronic, linear, and nonlinear optical properties of longer polyenes from a CNDO/SDCI calculation. The SCI, SDTCI results are also included for decapentaene.

			$\alpha(\omega;\omega)$ (in a.u.)			$\gamma(3\omega;\omega,\omega,\omega)$ (in 10^4 a.u.)			
N	$\hbar\omega$	$\Delta E(1\ ^1B_u)$	α_{xx}	α_{xy}	α_{yy}	γ_{xxxx}	γ_{xxyy}	γ_{yyxx}	γ_{yyyy}
					Decapentaene				
1	0.30	3.83	305.94	88.13	37.34	−3.352	−0.789	−0.745	−0.099
	0.65		312.91	90.05	37.92	−4.028	−1.022	−0.934	−0.122
	1.17		334.66	96.02	39.71	−13.409	−4.865	−3.875	−0.475
2	0.30	4.58	188.97	47.89	22.05	2.676	0.105	0.117	0.018
	0.65		191.94	48.58	22.26	3.366	0.128	0.133	0.020
	1.17		200.94	50.69	22.86	8.291	0.283	0.226	0.037
3	0.65	4.14	225.04	58.16	26.81	2.681	−0.021	−0.005	−0.002
	1.17		238.36	61.36	27.74	11.067	−0.005	−0.066	0.002
4	0.65	4.20	211.51	53.42	25.12	3.130	0.556	0.644	0.069
	1.17		223.45	56.21	25.93	10.939	2.282	1.038	0.230
					Polyene with 12 carbon atoms				
2	0.65	4.49	245.87	59.11	26.32	6.108	0.206	0.216	0.030
	1.17		257.81	61.74	27.04	16.028	0.474	0.388	0.055
					Polyene with 14 carbon atoms				
2	0.65	4.47	297.47	69.07	30.15	9.418	0.297	0.312	0.040
	1.17		311.93	72.15	30.96	25.106	0.687	0.579	0.074
					Polyene with 16 carbon atoms				
2	0.65	4.53	341.36	78.23	33.76	12.526	0.391	0.412	0.051

valence bond diagrams for generation and storage of configurations, but the one electron basis set is now selected from the Hartree–Fock molecular orbitals and the structures equivalent to the valence bond diagrams are referred to as molecular orbital spin pairing (MOSP) diagrams. The nonlinear optical properties reported in this paper have been calculated using the correction vector method. The method has been used to study the effect of correlations on the electronic and optical properties of finite conjugated polyenes containing not more than 16 carbon atoms. In the case of polyenes up to eight carbon atoms the electronic and optical properties have been calculated as a function of the order of CI, from SCI to FCI. In the case of 1,3,5,7,9-decapentaene calculations up to QCI ($n=4$) have been reported and in the case of longer polyenes the SDCI results are presented.

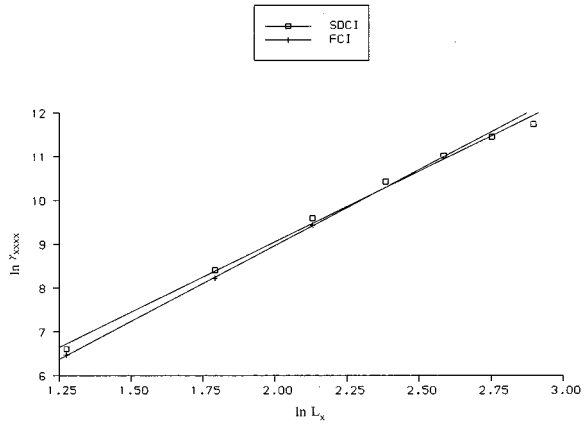

FIG. 6. A plot of $\ln[\gamma_{xxxx}(3\omega;\omega,\omega,\omega)]$ vs $\ln L_x$ at an excitation energy of 0.65 eV for all *trans* polyenes.

Our approach is novel in that it has incorporated an efficient method, derived from the diagramatic valence bond procedure, of generating a spin symmetry adapted basis set from configurations of arbitrary order of excitation between occupied and virtual MOs. A modified correction vector procedure which is much more efficient than the conventional SOS scheme for the computation of the NLO coefficient has been used. For the first time we report the effect of including excited configurations, in a systematic way, on the NLO coefficients of linear polyenes, thereby demonstrating the effect of electron correlations on the linear and nonlinear optical properties of low-dimensional conjugated systems.

From our calculations on smaller polyenes we conclude that, although SDCI reproduces most of the qualitative features of the electronic spectrum and gives the correct sign of the NLO coefficients, CI calculations of higher order have to performed to obtain reliable quantitative results. In these systems we have identified essential states contributing to the final value of the THG coefficient. The essential states are $1\ ^1A_g$, $1\ ^1B_u$, and $4\ ^1A_g$ for butadiene; $1\ ^1A_g$, $1\ ^1B_u$, and $5\ ^1A_g$ for hexatriene; $1\ ^1A_{1g}$, $1\ ^1E_{1u}$, and $5\ ^1E_{2g}$ for benzene; $1\ ^1A_g$, $1\ ^1B_u$, and $6\ ^1A_g$ for octatetraene. Only CI calculations for $n\geqslant 2$ reproduce, even approximately, the correct ordering of these states and the correct (positive) sign for the THG coefficient. In some cases there are significant differences in the values of the excitation energies when n is increased from 2 to 3 or 4. Both the ordering of the states and the sign of the THG coefficient from the SCI calculation are different from those obtained from calculations for $n>1$. The excitation energies of the low-lying states from the calculations are usually in very good agreement with the experimental and *ab initio* calculated values. The general feature to emerge from the calculations on the smaller polyenes is that to obtain a reliable estimate of the electronic and optical

properties of a polyene system of N carbon atoms one has to perform a CI calculation at least of the order of $N/2$.

From the calculations on longer polyenes, we conclude that the effect of higher excited configurations become more pronounced in these systems so that the SDCI calculation does not even reproduce the correct ordering of the electronic states. For example, the $1\,^1A_g$ state from the SDCI calculation of polyene of 16 carbon atoms lies above the $1\,^1B_u$ state, while it is generally accepted that the $1\,^1A_g$ state in longer polyenes lies below the ^1B_u state. However the sign of the THG coefficient of longer polyenes from the SDCI calculation is positive.

The potential advantage of the present method of choosing a CI basis set from the HF molecular orbitals, rather than from generalized valence bond configurations, is that, in the case of larger systems, it may enable various subsets of configurations to be systematically explored with a view to identifying a reasonable many-electron basis for the exploration of excited state properties in molecules of a particular type and size.

The computational features of the procedure described may also be of use in a wider range of CI studies, using *ab initio* or other semiempirical methods.

[1] R. Hubbard and G. Wald, J. Gen. Physiol. **36**, 269 (1952).
[2] V. Bonacic-Koutecky, P. Bruckmann, P. Hiberty, J. Koutecky, C. Laforestier, and L. Salem, Angew. Chem. Int. Ed. Engl. **14**, 575 (1978).
[3] *Handbook of Conducting Polymers*, edited by T. A. Skotheim (Marcel Dekker, New York, 1986), Vol. 1 and 2.
[4] W. A. Little, Phys. Rev. A **134**, 1416 (1964); A. F. Garito and A. J. Heeger, Acc. Chem. Res. **7**, 232 (1974).
[5] E. B. Yagnoskil, I. F. Shchegoler, V. N. Lanklin, P. A. Kononovich, M. V. Kartsonik, A. V. Zvanykirni, and L. I. Buranov, JETP Lett. **33**, 12 (1984).
[6] J. M. Williams, J. J. Emge, H. H. Wang, M. A. Beno, P. T. Cooper, L. N. Hall, K. D. Carlson, and G. W. Crabtree, Inorg. Chem. **23**, 2558 (1984).
[7] *Nonlinear Optical Properties of Organic Molecules and Crystals*, edited by D. S. Chemla and J. Zyss (Academic, Orlando, 1987).
[8] *Nonlinear Optical Properties of Organic and Polymeric Materials, ACS Symp Series*, edited by D. J. Williams (American Chemical Society, Washington, D.C., 1983), Vol. 233.
[9] In *Proceedings of the Materials Research Society, Nonlinear Optical Properties of Polymers*, edited by A. J. Heeger, J. Orenstein, and D. R. Ulrich (Society for Materials Research, Pittsburgh, 1988), Vol. 109.
[10] *Nonlinear Optical and Electroactive Polymers*, edited by P. N. Prasad and D. R. Ulrich (Plenum, New York, 1988).
[11] B. S. Hudson, B. E. Kohler, and K. Schulten, *Excited States*, edited by E. C. Lim (Academic, New York, 1982), Vol. 6, p. 1.
[12] B. A. Honig, A. Warshel, and M. Karplus, Acc. Chem. Res. **8**, 92 (1975).
[13] F. A. Matsen, Acc. Chem. Res. **11**, 387 (1978).
[14] M. F. Granville, G. R. Holtom, and B. E. Kohler, J. Chem. Phys. **72**, 4671 (1980).
[15] K. L. D'Amico, C. Manos, and R. L. Christiansen, J. Am. Chem. Soc. **102**, 1777 (1980).
[16] Z. G. Soos and S. Ramasesha, Phys. Rev. Lett. **51**, 2374 (1983).
[17] H. Thoman, L. R. Dalton, Y. Tomkeiwicz, N. J. Shiren, and T. C. Clarke, Phys. Rev. Lett. **50**, 553 (1983).
[18] P. Tavan and K. Schulten, J. Chem. Phys. **85**, 6602 (1986); Phys. Rev. B **36**, 4337 (1987); K. Schulten, I. Ohmine, and M. Karplus, J. Chem. Phys. **64**, 4422 (1976).
[19] S. Ramasesha and Z. Soos, J. Chem. Phys. **85**, 6602 (1986); **90**, 1067 (1989).
[20] I. D. L. Albert, J. O. Morley, and D. Pugh, J. Chem. Phys. **99**, 5197 (1993).
[21] J. R. Heflin, K. Y. Wong, O. Zamani-Kamiri, and A. F. Garito, Phys. Rev. B **38**, 1573 (1988).
[22] B. Pierce, J. Chem. Phys. **91**, 791 (1989).
[23] J. Del Bene and H. H. Jaffe, J. Chem. Phys. **48**, 1807 (1968); J. A. Pople and D. L. Beveridge, *Approximate Molecular Orbital Theory* (McGraw-Hill, New York, 1970); G. A. Segal, *Semiempirical Methods of Electronic Structure Calculation* (Plenum, New York, 1976).
[24] A. Szabo and N. S. Ostlund, *Modern Quantum Chemistry: An Introduction to Advanced Electronic Structure Theory* (MacMillan, New York, 1982); I. Shavitt, in *Methods of Electronic Structure Theory*, edited by H. F. Schaefer III (Plenum, New York, 1977), Chap. 6.
[25] D. Li, T. J. Marks, and M. A. Ratner, Chem. Phys. Lett. **131**, 370 (1986); D. Li, M. A. Ratner, and T. J. Marks, J. Am. Chem. Soc. **110**, 1704 (1988).
[26] S. J. Lalama and A. F. Garito, Phys. Rev. A **20**, 1179 (1979).
[27] C. W. Dirk, R. J. Tweig, and G. Wagniere, J. Am. Chem. Soc. **108**, 5387 (1986).
[28] V. J. Docherty, D. Pugh, and J. O. Morley, J. Chem. Soc. Faraday Trans. 2 **81**, 1179 (1985).
[29] E. N. Svendsen, C. S. Willand, and A. C. Albrecht, J. Chem. Phys. **98**, 5760 (1985).
[30] H. Sekino and R. J. Bartlett, J. Chem. Phys. **84**, 2726 (1986); **85**, 707 (1986).
[31] E. Perrin, P. N. Prasad, P. Mougenot, and M. Dupius, J. Chem. Phys. **91**, 4728 (1989).
[32] R. J. Cave and E. R. Davidson, J. Phys. Chem. **91**, 4481 (1987); Chem. Phys. Lett. **148**, 190 (1988).
[33] For a review of the CASSF method, see B. O. Roos, in *Ab Initio Methods in Quantum Chemistry-II*, edited by K. P. Lawley (Wiley, New York, 1987), p. 399.
[34] K. Andersson, P. A. Malmqvist, B. O. Roos, A. J. Sadlej, and K. Wolinski, J. Phys. Chem. **94**, 5483 (1990); K. Andersson, P. A. Malmqvist, and B. O. Roos, J. Chem. Phys. **96**, 1218 (1992).
[35] I. D. L. Albert, Ph.D. thesis, Indian Institute of Science, Bangalore, 1991.
[36] R. Pauncz, *Spin Eigen Function: Construction and Use* (Plenum, New York, 1979).
[37] S. Ramasesha and Z. G. Soos, Int. J. Quantum Chem. **25**, 1004 (1984).
[38] E. R. Davidson, J. Comput. Phys. **17**, 87 (1975).
[39] P. W. Langhoff, S. T. Epstein, and M. Karplus, Rev. Mod. Phys. **44**, 602 (1972).
[40] S. Ramasesha, J. Comput. Chem. **11**, 545 (1990).
[41] I. D. L. Albert and S. Ramasesha, Chem. Phys. Lett. **182**, 351 (1991).
[42] O. A. Mosher, W. M. Flicker, and A. Kuppermann, J. Chem. Phys. **59**, 6502 (1973).
[43] R. McDiarmid, Chem. Phys. Lett. **34**, 130 (1975).
[44] L. S. Andres, M. Merchan, I. N. Gil, R. Lindh, and B. O. Roos, J. Chem. Phys. **98**, 3151 (1993).
[45] R. R. Chadwick, M. Z. Zgierski, and B. S. Hudson, J. Chem. Phys. **95**, 7204 (1991).
[46] W. J. Buma, B. E. Kohler, and K. Song, J. Chem. Phys. **92**, 4622 (1990); **94**, 6367 (1991).
[47] T. Fujii, A. Kamata, M. Shimuzu, Y. Adachi, and S. Maeda, Chem. Phys. Lett. **115**, 492 (1985).
[48] E. N. Lassetre, A. Skerbele, M. A. Dillon, and K. J. Ross, J. Chem. Phys. **48**, 5066 (1968).
[49] L. S. Andres, R. Lindh, B. O. Roos, and M. Merchan, J. Phys. Chem. **97**, 9360 (1993).